nature communications

Article

https://doi.org/10.1038/s41467-025-58504-z

Intranasal influenza virus-vectored vaccine offers protection against clade 2.3.4.4b H5N1 infection in small animal models

Received: 22 August 2024

Accepted: 21 March 2025

Published online: 01 April 2025

Check for updates

Ying Liu[1,2,4], Shaofeng Deng[1,2,4], Shuang Ren[1,2], Rachel Chun-Yee Tam[1,2], Siwen Liu[1,2], Anna Jinxia Zhang[1,2], Kelvin Kai-Wang To[1,2,3], Kwok-Yung Yuen[1,2,3], Honglin Chen[1,2] ✉ & Pui Wang[1,2] ✉

The highly pathogenic avian influenza (HPAI) H5N1 virus has been endemic in aquatic birds since 1997, causing outbreaks in domestic poultry and occasional human infections worldwide. Recently, the cross-species transmission of a new reassortant variant from clade 2.3.4.4b of H5N1 to cattle in the US has heightened concerns regarding the expansion of host range and potential human infection. As eradicating the H5N1 virus from its reservoir is impossible, it is essential to prepare for a potential pandemic caused by an H5N1 derivative. Utilizing a deleted-NS1 live attenuated influenza viral vector vaccine system (DelNS1 LAIV), a system we have previously used in the development of a COVID-19 vaccine, we have rapidly developed an intranasal vaccine for cattle H5N1 and related clade 2.3.4.4b strains, based on publicly available sequences. Our research demonstrates that a single intranasal immunization can provide effective protection against lethal challenges from HPAI cattle or mink H5N1 variants, offering strong, sustained immunity after two months in female mouse and male hamster models. Immunogenicity analysis reveals that intranasal vaccination with DelNS1 LAIV induces robust neutralizing antibody, mucosal IgA and T cell responses in mice. It is crucial to further evaluate the DelNS1-H5N1 LAIV system to prepare for potential future H5N1 outbreaks in humans.

The highly pathogenic avian influenza (HPAI) virus H5N1 first emerged in 1996 and caused a human outbreak in Hong Kong in 1997, resulting in 18 infections and 6 deaths[1]. The outbreak was controlled after millions of chickens were culled in Hong Kong. However, the descendants of the 1996 H5N1 virus (Gs/Guangdong/96) have continued to evolve, undergoing complex reassortment events with low pathogenicity avian influenza viruses, such as H9N2. This led to outbreaks in domestic poultry and sporadic human infections in several Southeast Asian countries during 2004–05[2,3]. A major outbreak in migratory birds in Qinghai Lake, China, resulted in the spread of avian H5N1 virus from Southeast Asia to Europe[4]. The persistent endemicity of H5N1 virus in wild birds has led to global dissemination and increasing incidences of crossing of host barriers to infect various mammalian species[5,6]. Most recently, the clade 2.3.4.4b avian H5N1 virus caused a major outbreak in farmed minks in Europe in 2022[7]. Another reassortant clade 2.3.4.4b variant has been circulating in North America, causing infections of dairy cattle in the US since early 2024[8,9]. Although human infections with these H5N1 variants are still sporadic and

[1]State Key Laboratory for Emerging Infectious Diseases and Department of Microbiology, Li Ka Shing Faculty of Medicine, The University of Hong Kong, Pokfulam, Hong Kong Special Administrative Region, China. [2]Centre for Virology, Vaccinology and Therapeutics Limited, The University of Hong Kong, Pokfulam, Hong Kong Special Administrative Region, China. [3]Pandemic Research Alliance Unit, The University of Hong Kong, Pokfulam, Hong Kong Special Administrative Region, China. [4]These authors contributed equally: Ying Liu, Shaofeng Deng. ✉e-mail: hlchen@hku.hk; puiwang@hku.hk

human-to-human transmissions have not been reported[10], respiratory droplet transmission has been observed in studies using mammalian models[11]. The altered tissue tropism for a greater range of mammalian species has raised major concerns regarding the evolutionary pathway of clade 2.3.4.4b viruses towards human infections[8,12]. Structural analysis of the hemagglutinin of H5N1 isolated from cattle revealed that a single mutation in the receptor binding region could switch receptor binding specificity to recognize human receptors[13,14]. It is noteworthy that in a recent human case identified in British Columbia, substitutions enhancing human receptor specificity were found in the key receptor binding residues (E190D and Q226H, H3 numbering) in the hemagglutinin of the 2.3.4.4b H5N1 virus[15].

HPAI viruses mainly arise from H5 and H7 subtypes of avian influenza viruses. In 2013, a reassortant avian H7N9 virus caused a major outbreak in China[16]. However, after the implementation of massive vaccination in poultry, the outbreaks of H7N9 were controlled, and virus activity has since remained at very low levels following the five waves of epidemics affecting China from 2013-2017[17–19]. In contrast to the avian H5N1 virus, global dissemination of avian H7N9 virus has not occurred. Although poultry vaccination strategies were employed for H5 virus as early as 2004[18], the HPAI H5 subtype virus has become endemic in many regions and continues to circulate globally, expanding its host range. The genomic flexibility for frequent reassortment with other low pathogenicity avian influenza viruses and the adaptation to cause asymptomatic infection among some wild migratory birds appear to provide a unique opportunity for the H5 virus to establish long-term endemicity in migratory birds. Consistent with this assumption, the 2013 avian H7N9 virus was not reported to be detected in migratory birds. It is impossible to eradicate H5 subtype avian influenza viruses from migratory birds, and vaccination of domestic poultry does not (provide sterilizing immunity to prevent infection but rather only reduces virus shedding and transmission to achieve a certain degree of control[20,21]. The long-time endemicity of H5 virus provides opportunities for the virus to interact with various hosts, accumulate adaptative mutations, and optimize its genome constellation, making it one of the most likely potential pandemic subtypes if additional conditions that enable efficient transmission in humans become available. Given the ability of current clade 2.3.4.4b H5 subtype viruses to infect various mammalian species, it is necessary to prepare for a potential outbreak in humans. High-efficiency replication of clade 2.3.4.4b H5 subtype viruses in infected animals has been observed[12], suggesting an accumulation of replication fitness for H5 virus in avian and mammalian cells. Developing vaccines for urgent use in a pandemic can take almost one year after human-to-human transmission is observed to time to deployment (including clinical trials), as evidenced in the COVID-19 pandemic[22], even when benefited by the application of multiple vaccine technology platforms. While the mRNA vaccine approach has revolutionized the production of vaccines for emerging viruses, more vaccine strategies are needed for preparedness for potential future influenza pandemics.

We have developed a system consisting of a panel of live attenuated influenza viruses by deleting NS1 from influenza virus genomes and introducing adaptative mutations for replication in eggs and MDCK cells[23]. The resulting deleted-NS1 live attenuated influenza viral vectors (DelNS1 LAIV) are safe and able to induce both systemic and mucosal immunity through intranasal immunization[24]. Based on publicly available sequences of clade 2.3.4.4b cattle and mink H5N1 viruses, we have generated two DelNS1-H5N1 live attenuated vaccine candidates. We have demonstrated that the DelNS1 viral vectored H5N1 vaccines are avirulent in mice and hamsters and that a single intranasal immunization dose provides effective protection against lethal challenges from HPAI H5N1 cattle and/or mink variants in these animal models. Further testing reveals that the DelNS1-H5N1 vaccines offer comprehensive and lasting immunity in mice.

Results

DelNS1 live attenuated viral vectored H5N1 vaccines are highly immunogenic

In our previous study, we described a panel of influenza viral vectors that carry a deletion of the NS1 gene from the NS segment and contain adaptive mutations to support replication in MDCK and egg cells[23]. This panel of DelNS1 viral vectors can be used to create live attenuated influenza vaccines (LAIVs) for influenza or to express other antigens from the NS1 site to induce an immune response against other respiratory viruses, such as coronaviruses[24]. To generate the DelNS1-H5N1 live attenuated vaccines, we synthesized H5 and N1 genes based on publicly available sequences of the clade 2.3.4.4b cattle and mink H5N1 viruses[25,26]. We removed the polybasic cleavage motif, which is considered to be a virulence factor of highly pathogenic avian influenza (HPAI) H5N1 viruses, from the synthesized H5 hemagglutinins. We then constructed and rescued DelNS1-cH5N1 (with cattle H5 and N1) and DelNS1-mH5N1 (with mink H5 and N1) LAIVs in MDCK cells with the remaining six viral segments being from the CA4-DelNS1 (2009 H1N1) backbone (Fig. 1A). Both DelNS1-cH5N1 and DelNS1-mH5N1 LAIVs can replicate well in MDCK cells and embryonated chicken eggs (Fig. 1B). When continuously passaged in either culture system, the genomes of the DelNS1-H5N1 LAIVs remained stable, sequencing analysis revealed a single nucleotide substitution in the NA gene of DelNS1-cH5N1 (NA-T423C) from passage 5, which did not result in an amino acid change (NA-141N). No other mutation was detected in the genomes DelNS1-mH5N1 virus after 10 passages. These findings demonstrate the high genetic stability of the DelNS1 viruses during serial passaging, suggesting their potential suitability for further development as vaccine candidates or viral vectors. Importantly, the DelNS1-H5N1 LAIVs were avirulent in mice and hamsters that were inoculated with a high titer of either cattle or mink (mice) or cattle only (hamsters) DelNS1-H5N1 vaccine candidate (Figs. 1C and S1A). No vaccine virus shedding was detected in nasal turbinates from inoculated animals, and no virus was detected in lungs or brain tissues of either species, or livers (hamsters only), from day 2 to day 6 post immunization (Figs. 1D and S1B). Histopathological analysis of mouse tissues revealed only minor immune activation in lungs and nasal turbinate post inoculation, with no other pathological changes related to infection was found (Fig. S2). These mild and temporary inflammations represent signs of immune response triggered by the DelNS1-H5N1 LAIV vaccine in the lung and nasal turbinate tissues.

In preparing for a potential pandemic, it is crucial to develop vaccines that can be used to respond swiftly to human outbreaks and control human-to-human transmission. Current influenza vaccines are primarily made from split inactivated virions and are administered through intramuscular injection. For a host immune-naïve to H5N1 virus infection, two doses of adjuvanted vaccination may be needed to induce sufficient antiviral immunity[27,28]. It is critical to have a vaccine that is highly immunogenic and can be administered as a single dose to induce effective immunity, particularly mucosal immunity, to prevent or slow down human transmission in response to an emerging influenza virus. To test whether the DelNS1-H5N1 LAIVs might be useful as vaccines for a rapid response to an outbreak, we evaluated the immunogenicity of a single dose of either DelNS1-cH5N1 or DelNS1-mH5N1 LAIV in mouse and hamster (DelNS1-cH5N1 only) models (Fig. 2A). DelNS1-H5N1 LAIVs derived from either cattle or mink H5N1 viruses induced anti-H5 antibodies within three weeks of immunization, as shown in ELISA assays (Figs. 2B and S1C). Neutralization assays with cattle or mink H5N1 live virus confirmed that a single immunization dose induced strong virus-neutralizing antibody responses in mice and hamsters (Figs. 2C and S1C). Immunization with second dose of vaccine further enhances the neutralizing antibodies in hamsters (Fig. S1D). The

https://doi.org/10.1038/s41467-025-58504-z

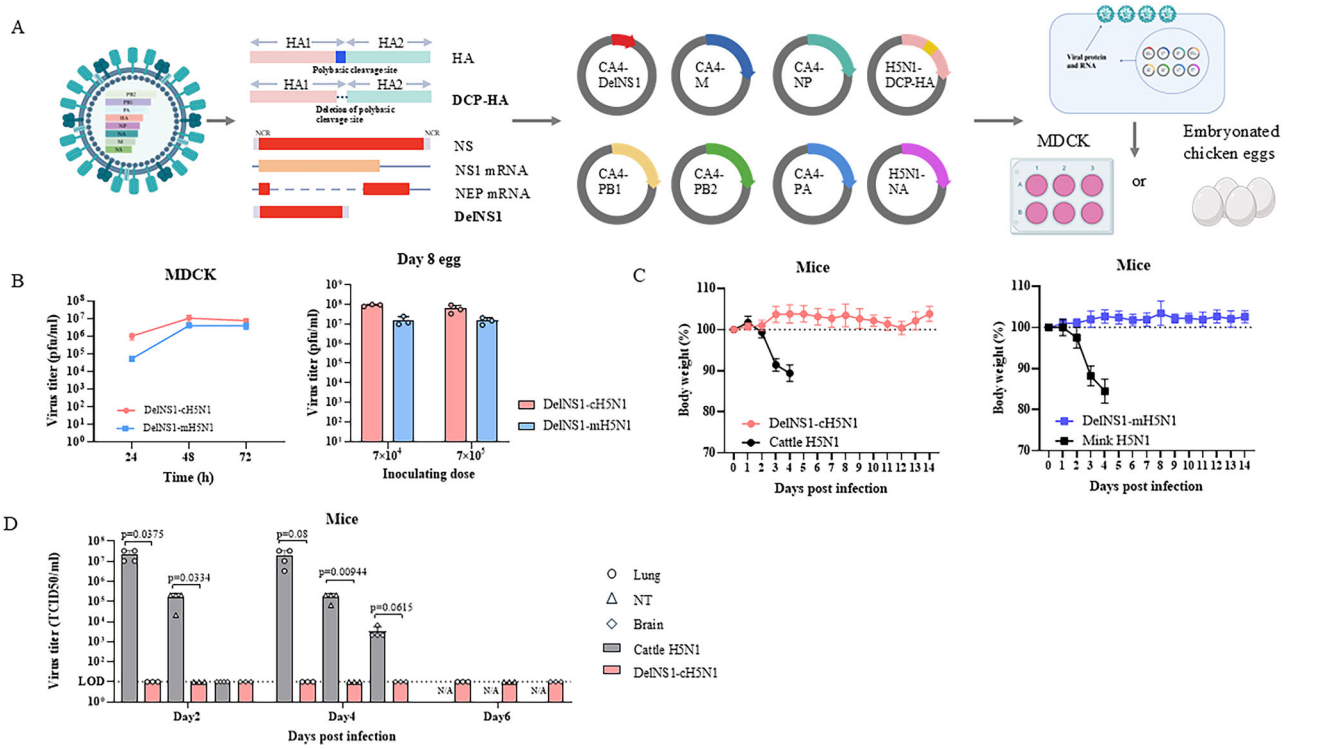

Fig. 1 | Generation and characterization of DelNS1-H5N1 vaccines. A Illustration of construction and generation of DelNS1-H5N1 vaccines. NCR, non-coding region. DCP: deletion of polybasic cleavage site. **B** Growth kinetics of DelNS1-cH5N1 and DelNS1-mH5N1 at 33 °C were analyzed in MDCK cells inoculated at a multiplicity of infection (MOI) of 0.01 ($n = 3$), and viral titers of DelNS1-cH5N1 and DelNS1-mH5N1 were measured in day 8 embryonated chicken eggs 48 h after inoculation with different initial doses ($n = 3$). Viral supernatants or allantoic fluids were collected and titrated by plaque assay in MDCK cells. **C** Virulence of DelNS1-cH5N1 and DelNS1-mH5N1 was examined in mice. Mice were inoculated intranasally with DelNS1-cH5N1 (10^6 pfu, $n = 8$) or cattle H5N1 (5000 pfu, $n = 8$), DelNS1-mH5N1 (10^6 pfu, $n = 8$) or mink H5N1 (10^4 pfu, $n = 8$). Body weights were observed for 14 days. **D** Mice were inoculated intranasally with DelNS1-cH5N1 (10^6 pfu, $n = 3$) or cattle H5N1 (5000 pfu, $n = 4$), with virus titers in lungs, nasal turbinates (NT) and brain tissues of mice being examined at day 2, day 4 and day 6 post infection. LOD limit of detection. Data represents mean values ± standard deviation (SD) of results. N/A not available. Statistical comparisons between means were performed by Student's *t*-test (two-tailed). Cartoons were created in BioRender. Wang, P. (2025) https://BioRender.com/n81t049. Source data are provided as a Source Data file.

unique advantage of the DelNS1 LAIV system is the intranasal immunization route, which induces both mucosal and systemic immunities. Vaccine-induced IgA in the respiratory tract is important for the prevention of infection and reducing transmission. However, vaccines administered via intramuscular injection induce limited mucosal immunity[29,30]. It is recommended that development of next generation vaccines for respiratory viruses should also focus on their ability to induce robust mucosal immunity. The measurement of mucosal immunity is challenging due to the difficulty of collecting specimens from the nasal tract. Specimens collected from bronchoalveolar lavage (BAL) and nasal washes were analyzed in this study. We showed that both DelNS1-cH5N1 and DelNS1-mH5N1 LAIVs can induce virus-specific IgA detectable in the bronchoalveolar lavage (BAL) fluids and nasal washes of immunized mice (Fig. 2D–E). Cellular immunity is another line of antiviral immunity that plays an important role in clearing viruses. We analyzed both peripheral and lung resident T cells in immunized mice. To study tissue resident T cells in mice, we first labelled circulating immune cells through intravenous injection of CD45-specific antibody. Using NP tetramers and intracellular cytokine staining we showed that our DelNS1-H5N1 LAIVs induced influenza A NP-specific CD8+ and CD4+ T cells in the lungs and spleen tissues of immunized mice (Fig. 3). More importantly, our results show that CD69+ CD103+ tissue resident memory T cells were induced in the DelNS1-H5N1 LAIV immunized mice, suggesting DelNS1-H5N1 LAIV immunization induces tissue resident memory T cell immunity to influenza A virus. It is noted that immunization with DelNS1-H5N1 through the intranasal route induces greater $CD8^+$ T cells responses in the lungs than in the spleen.

The DelNS1-H5N1 vaccines provide effective protection against lethal challenge with H5N1 virus

We evaluated the protective efficacy of the DelNS1-H5N1 LAIV vaccines in a H5N1 virus challenge experiment. We constructed reverse genetic versions of mink and cattle H5N1 viruses for use in animal challenge experiments (detailed information can be found in Materials and Methods). Both viruses replicate efficiently in MDCK and A549 cells (Fig. S3A, B). Consistent with published reports[8,12], we showed that both cattle and mink H5N1 viruses were highly pathogenic to mice, with the cattle H5N1 virus ($MLD_{50} = 1$ pfu) appearing to be much more virulent than the mink H5N1 virus ($MLD_{50} = 1000$ pfu) (Fig. S3C–D, F–G). Challenge with reverse genetic version of cattle or mink H5N1 virus led to infection of multiple organs in mice (Fig. S3E, H). To evaluate the protective effect of DelNS1-H5N1 LAIV vaccines, mice and hamsters were immunized once with either DelNS1-cH5N1 or DelNS1-mH5N1 (mice only) LAIV vaccines via intranasal drop (10^6 pfu). Immunized animals were then challenged with either cattle H5N1 (5000 pfu) or mink H5N1 (10^4 pfu – mice only) reverse genetically constructed H5N1 virus at four weeks after vaccination (Fig. 4A). While mock-immunized mice died within one week of virus challenge with virus present in lungs, nasal turbinates and brain at 4 dpi, immunized mice challenged with homologous virus showed no apparent disease throughout the two weeks of observation and no virus was detected in the sampled tissues (Fig. 4B, C). In the hamster challenge experiment, while animals showed slight body weight loss

https://doi.org/10.1038/s41467-025-58504-z

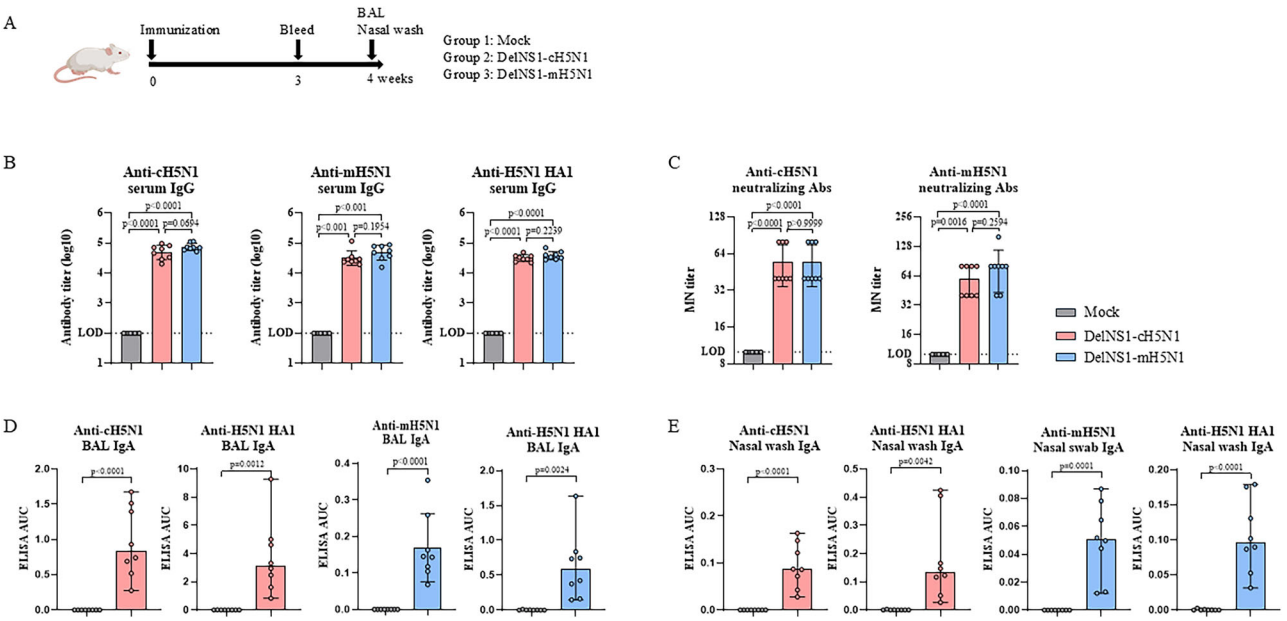

Fig. 2 | Immunogenicity evaluation of DelNS1-H5N1 vaccines. A Schedule of immunization, blood collection, and bronchoalveolar lavage (BAL) fluid and nasal wash collection from BALB/c mice. Mice ($n = 8$ for each group) were intranasally immunized with 10^6 pfu DelNS1-cH5N1 or 10^6 pfu DelNS1-mH5N1, or mock-immunized (PBS). **B** At week 3, serum were collected and tested for IgG titers against the cH5N1 (DelNS1-cH5N1) virus, mH5N1 (DelNS1-mH5N1) virus, or H5N1-HA1 protein. **C** Microneutralization (MN) titers were measured against live viruses. At week 4 post immunization, mice from all groups were sacrificed and BAL and nasal wash samples collected. **D** BAL IgA levels and **E** nasal wash IgA levels against cH5N1, mH5N1, or H5N1-HA1 were measured. LOD: limit of detection. Data represents the mean values ± SD of results. Statistical analysis was performed for (**B**) and (**C**) using one-way ANOVA followed by Dunn's multiple comparisons test. Statistical analysis was performed for (**D**) and (**E**) using Student's *t*-test (two-tailed). The mouse cartoon was created in BioRender. Wang, P. (2025) https://BioRender.com/n83i107. Source data are provided as a Source Data file.

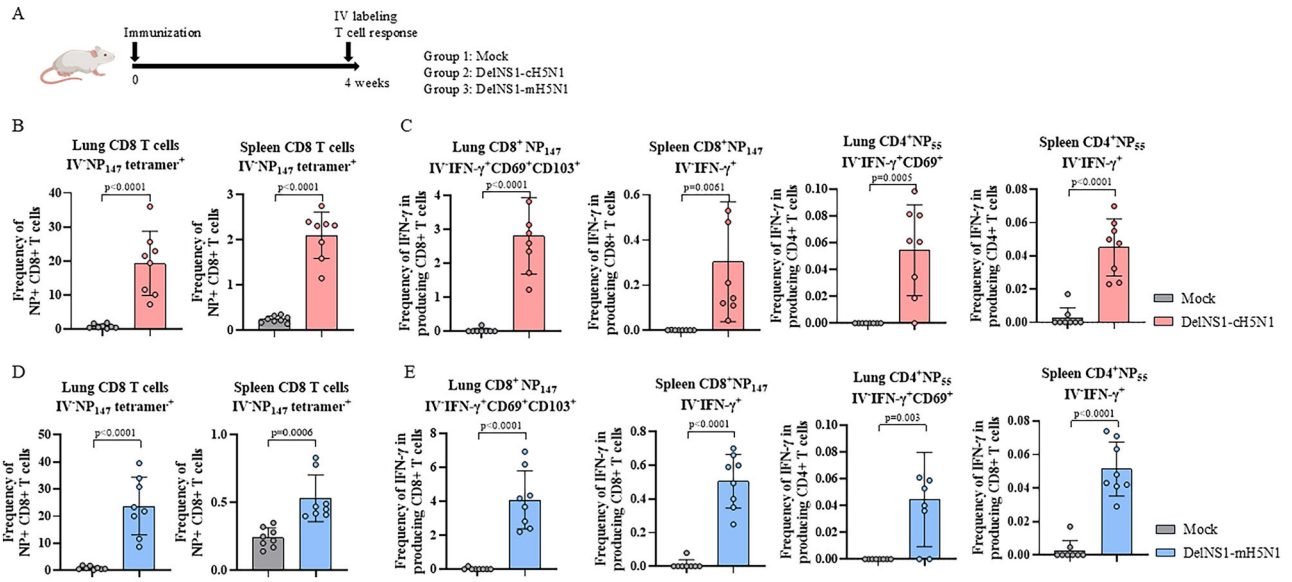

Fig. 3 | DelNS1-H5N1 vaccines induce CD4+ and CD8+ T cell responses. **A** Schedule for immunization of BALB/c mice. At week 4 after immunization, 2 μg of PE-Cy5 conjugated CD45-specific antibody was injected intravenously via the tail vein 5 min before sacrifice ($n = 8$ for each group). **B** Lung cells and splenocytes were obtained and stained with Zombie, anti-CD8 and NP_{147} tetramer. Flow cytometry gating was performed to assess the frequency of live DelNS1-cH5N1-induced non-circulating (IV CD45-PE-Cy5 negative) NP-specific CD8+ T cells among lung cells and splenocytes (percentage IV-CD8 + NP_{147} tetramer+ out of all live IV-CD8+ T cells). **C** Lung or spleen cells were stimulated with NP_{147} or NP_{55} peptide overnight. Surface markers (CD69, CD103, CD4, CD8 and Zombie) were stained, followed by fixation, permeabilization, and intracellular staining for IFN-γ. DelNS1-cH5N1 induced tissue-resident memory cells in lungs and spleens were displayed (IV-IFNγ + CD69 + CD103 + CD8 + T cells and IV-IFNγ+CD69+CD4+ T cells out a percentage of all live IV- CD8+ and CD4+ T cells, respectively). **D** DelNS1-mH5N1 induced non-circulating T cells in lung cells and spleens (IV-CD8 + NP_{147} tetramer out of all live IV-CD8 T cells). **E** DelNS1-mH5N1 induced tissue-resident memory cells in lungs and spleen were displayed (IV-IFNγ+CD69+ CD103+CD8+ T cells and IV-IFNγ + CD69+ CD4+ T cells out a percentage of all live IV- CD8+ and CD4 + T cells, respectively). Data represents the mean values ± SD of results. Statistical comparisons between means were performed by Student's t-test (two-tailed). The mouse cartoon was created in BioRender. Wang, P. (2025) https://BioRender.com/n83i107. Source data are provided as a Source Data file.

https://doi.org/10.1038/s41467-025-58504-z

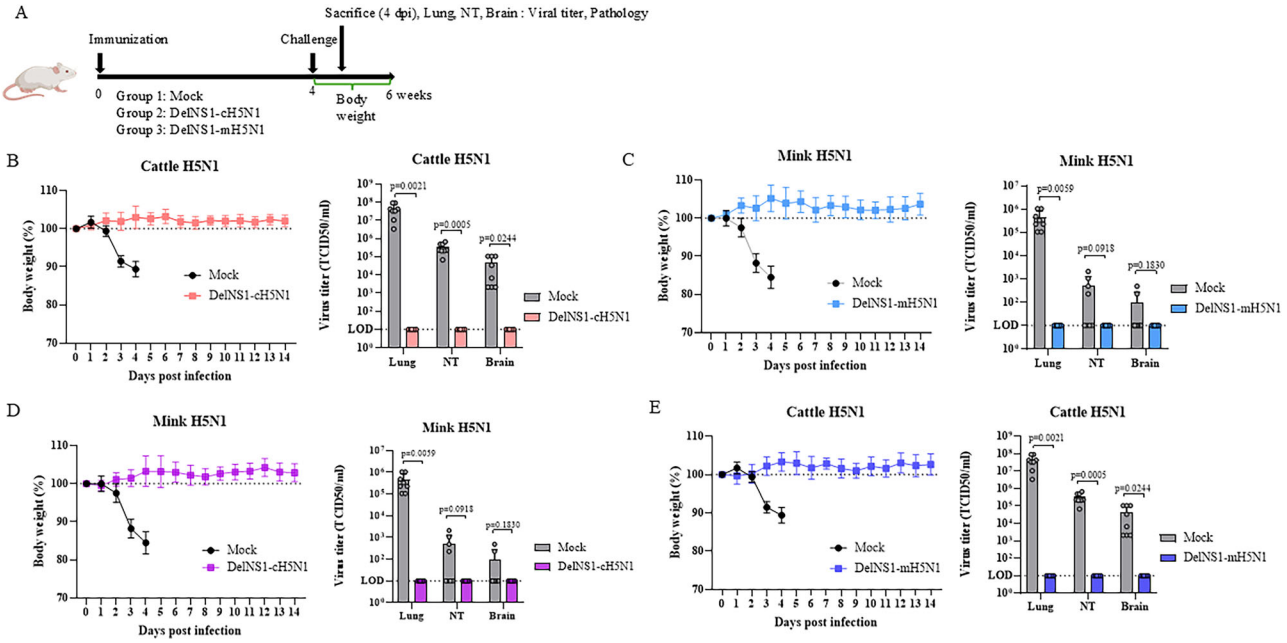

Fig. 4 | DelNS1-H5N1 vaccines provide protection against different 2.3.4.4b clade viruses. A Illustration of schedule of immunization, virus challenge and sacrifice for BALB/c mice. Mice were intranasally vaccinated with DelNS1-cH5N1 (10^6 pfu, $n = 32$, two independent experiments), DelNS1-mH5N1 (10^6 pfu, $n = 32$, two independent experiments) or mock-vaccinated ($n = 16$, two independent experiments), then challenged with either cattle H5N1 virus (5000 pfu) or mink H5N1 virus (10^4 pfu) 4 weeks after immunization. **B** Mice immunized with DelNS1-cH5N1 and challenged with cattle H5N1 virus; body weights were monitored for 14 days and viral titers in the lungs, NT and brain were measured at 4 dpi. **C** Mice immunized with DelNS1-mH5N1 and challenged with mink H5N1 virus; body weights were monitored for 14 days and viral titers in the lungs, NT and brain were measured at 4 dpi. **D** DelNS1-cH5N1-vaccinated mice were challenged with mink H5N1 virus, and body weights monitored for 14 days and viral titers in the lungs, NT and brain measured at 4 dpi. **E** DelNS1-mH5N1-vaccinated mice were challenged with cattle H5N1, and body weights monitored for 14 days and viral titers in the lungs, NT and brain measured at 4 dpi. LOD: limit of detection. Data represents mean values ± SD of results. Statistical comparisons between means were performed by Student's *t*-test (two-tailed). Mouse cartoon was created in BioRender. Wang, P. (2025) https://BioRender.com/n83i107. Source data are provided as a Source Data file.

but recovered quickly and virus was detected in the lungs of one animal (1/4) with single dose of vaccination, all vaccinated hamsters were completely protected (Fig. S1E, F). In the control group without vaccination, 7/8 hamsters died within 8 days of infection while one hamster recovered after losing nearly 20% of its body weight (Fig. S1E). It is noted that two doses of vaccination achieved optimal protection, and no virus was detected in the lungs and other organs of animals (Fig. S1E, F). There are many sequence variations between the H5 genes of cattle and mink H5N1 viruses, and some of these variations are located in the antigenic regions. However, we found that immunization with either DelNS1-cH5N1 or DelNS1-mH5N1 LAIV can provide cross-protection against challenge with reverse genetic versions of mink or cattle H5N1 virus respectively (Fig. 4D, E), suggesting that immunization with DelNS1-H5N1 LAIVs induce cross-protective immunity against viruses in the same clade. More importantly, we found that immunization with DelNS1-H5N1 LAIVs not only protects against death and disease (body weight loss) but also induces mucosal immunity in the respiratory tissues to prevent virus replication in the airway, as no virus was detected in either lungs or nasal turbinates of immunized mice following virus challenge (Fig. 4). This evidence further strengthens the argument that immunization with DelNS1-H5N1 LAIVs induces comprehensive protective immunity against H5N1 virus infection.

Histopathological analyses of lung tissues from immunized and mock-vaccinated groups of mice after H5N1 virus challenge confirmed vaccine protective efficacy in mice and hamsters (Fig. S4). In the control groups without vaccination, severe bronchiolar epithelial depletion, diffuse alveolar wall edema, and alveolar wall immune infiltration were observed. Consistent with the result of the pathogenicity experiment, the cH5N1-challenged group appears to have a more severe pathological presentation than that of mH5N1-infected mice. In contrast, normal histological structure and only relative mild peribronchiolar immune cell infiltration was observed in vaccinated mice after challenge with either of the H5N1 viruses. Analysis of nasal turbinate pathology showed segmentally distributed epithelial cell damage, with the nasal cavities of H5N1-challenged unimmunized mice containing large amounts of detached epithelium and cell debris (Fig. S5). Neural dissemination is one of the unique features of highly pathogenic avian H5N1 influenza virus infection. Pathological analysis confirmed that DelNS1-H5N1 vaccination effectively protected challenged mice from any signs of disease in the brain (Fig. S6). One of the major mechanisms leading to the highly pathogenic properties of avian H5N1 infection in humans is the induction of an aberrant pro-inflammatory cytokine response, or so-called cytokine storm[31,32]. In contrast to the mock-immunized mice, we found that mice immunized with either DelNS1-cH5N1 or DelNS1-mH5N1 LAIV vaccines were generally well protected against this event and for the most part did not express elevated pro-inflammatory cytokines in the lungs after H5N1 virus challenge (Fig. 5).

DelNS1-H5N1 LAIV immunization in the presence of pre-existing immunity to influenza

Since DelNS1-H5N1 LAIVs are administered through the nasal route, there is a possibility that prior infection with other influenza viruses, such as seasonal flu, may impact the ability of the vaccine to provoke an immune response and affect its protective efficacy. To investigate this issue, we infected mice with a combination of H3N2 and H1N1 DelNS1 LAIVs four weeks before immunization with one of the DelNS1-H5N1 LAIVs (Fig. 6, DelNS1-mH5N1). The mice were later challenged with a lethal dose of reverse genetic version of mink H5N1 virus. The experiment showed that prior infection-induced antibodies to H1N1 and H3N2 viruses, but did not affect the induction of anti-H5N1

https://doi.org/10.1038/s41467-025-58504-z

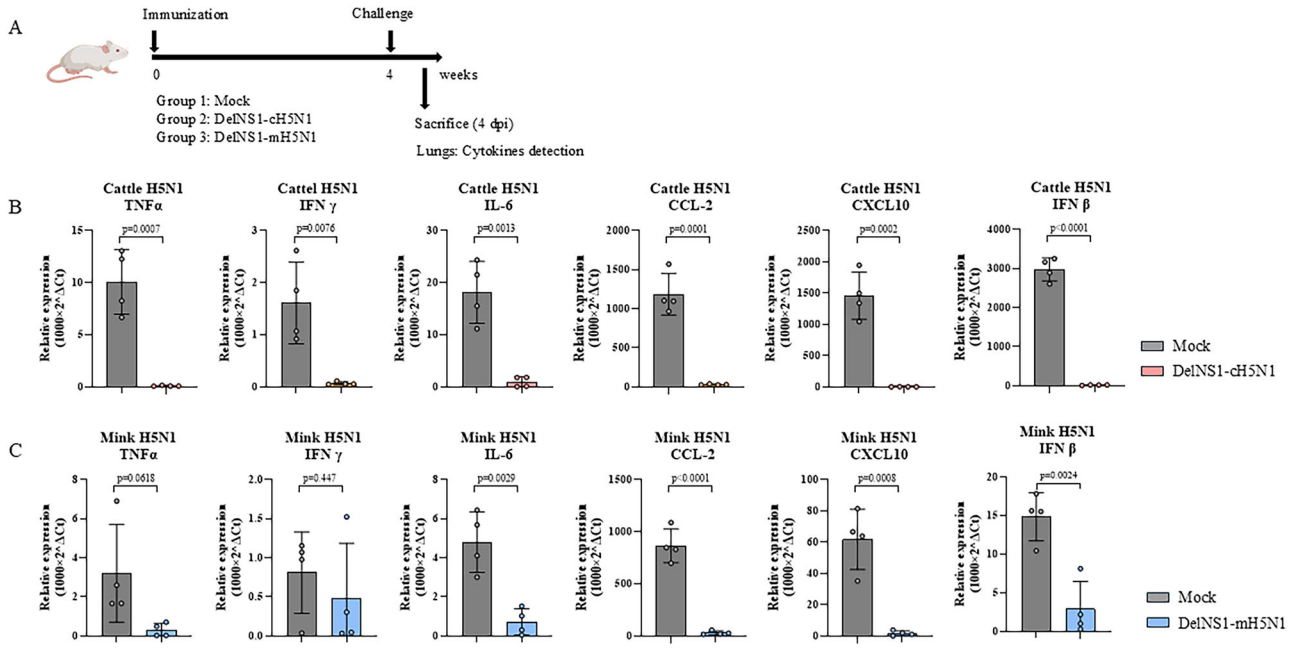

Fig. 5 | Immunization reduces expression of pro-inflammatory genes in mice post-challenge. A Illustration of schedule of immunization, virus challenge and sacrifice for BALB/c mice. **B** Mice were intranasally vaccinated with DelNS1-cH5N1 (10^6 pfu), or PBS ($n = 4$ for each group), then challenged with cattle H5N1 virus (5000 pfu) 4 weeks after immunization. Pro-inflammatory genes were measured by RT-qPCR after isolation of RNA from lungs at 4 dpi. **C** Mice were intranasally vaccinated with DelNS1-mH5N1 (10^6 pfu), or PBS ($n = 4$ for each group), then challenged with mink H5N1 virus (10^4 pfu) 4 weeks after immunization. Pro-inflammatory genes were measured by RT-qPCR after isolation of RNA from lungs at 4 dpi. Data represent mean values ± SD of results. Statistical analysis was performed using Student's *t*-test (two-tailed). The mouse cartoon was created in BioRender. Wang, P. (2025) https://BioRender.com/n83i107. Source data are provided as a Source Data file.

immunity (both neutralizing antibodies and T cell immunity) by subsequent immunization with the DelNS1-H5N1 LAIV (Fig. 6D). These results indicate that pre-existing immunity to seasonal influenza virus does not disrupt the immune response induced by immunization with DelNS1-H5N1 LAIV in mice. Furthermore, the mice were effectively protected against lethal challenge with the reverse genetic version of mink H5N1 virus, with no virus detected in the lungs and nasal turbinate tissues of immunized mice (Fig. 6E).

The study also demonstrated that immunization with the DelNS1-H5N1 LAIVs induced CD69+CD103+ tissue resident memory T cells (Fig. 3 & Fig. 6), which play a crucial role in adaptive immunity against reinfection. To determine if the DelNS1-H5N1 LAIV vaccines may induce lasting memory immunity, we tested mice at 8 weeks post immunization, finding them to still have significant levels of anti-H5N1 virus neutralizing antibodies and BAL IgA (Fig. 7A-B, D). Significantly, these mice were still protected against lethal challenge with H5N1 virus (Fig. 7C, E), suggesting that DelNS1-H5N1 LAIV immunization may induce sustained immunity even after just one dose. Further studies are needed to validate the sustainment of immunity to H5N1 virus in humans. To further validate and titrate the protective effect of the DelNS1-H5N1 LAIV vaccines, we immunized mice with a lower dose (1/5 of the original dose) of the DelNS1-mH5N1 and DelNS1-cH5N1 LAIV vaccines. We found that the lower vaccination dose induced a comparable level of antibodies in mice to the original dose and effectively protected mice from lethal challenge with H5N1 virus (Fig. S7). Taken together, our results demonstrate that DelNS1-H5N1 LAIVs are highly immunogenic in mice, being unaffected by existing immunity induced by prior influenza virus infection, and that one dose of intranasal immunization is sufficient to induce comprehensive systemic and mucosal immunity and provide highly effective protection against lethal challenge with H5N1 virus in this model.

Discussion

The unprecedented persistent circulation and expansion of host range by the avian H5N1 virus has raised significant concerns in recent years[33]. There are fears that the continual evolution and accumulation of mutations for mammalian adaptation, or reassortment with seasonal influenza viruses, by the current avian H5N1 virus might increase the likelihood of human transmission and foster a new pandemic. Each pandemic is unique, and it is impossible to predict their timing, or the type of pathogen involved. Stockpiling vaccine technology is a major strategy for pandemic preparedness. Effective vaccines are the most efficient way to minimize mortality and morbidity, as well as to reduce transmission in outbreaks caused by emerging viruses[34–36]. It is essential to test and evaluate various technology platforms for the rapid deployment of vaccines for a potential H5N1 virus outbreak. The mRNA technology has shown a unique advantage in the deployment of vaccines for COVID-19 and is also being investigated for the H5N1 virus[37]. Studies have revealed that while mRNA vaccines are effective in inducing a systemic immune response, they are less effective in preventing virus shedding in the nasal turbinates[29,30,37]. The development of effective vaccines that can induce both systemic and mucosal immunity is considered to be the focus of the next generation of vaccines for respiratory viruses. This study describes an intranasal influenza virus-vectored vaccine that provides both systemic and mucosal immunity against H5N1 infection in mice and hamsters. The DelNS1 live attenuated influenza viral vaccine (LAIV) system is based on an influenza viral vector with the key virulence element, NS1, deleted from the NS segment of the viral genome[23,38]. While an influenza virus without NS1 does not replicate in interferon-competent cells, we identified adaptive mutations in the M and other segments that enable the DelNS1 LAIV to replicate in MDCK cells and embryonated eggs, both of which are existing systems for influenza vaccine production[23,38]. The DelNS1-H5N1 LAIV vaccine replicates well in these systems and shows no apparent virulence in a mouse and hamster

https://doi.org/10.1038/s41467-025-58504-z

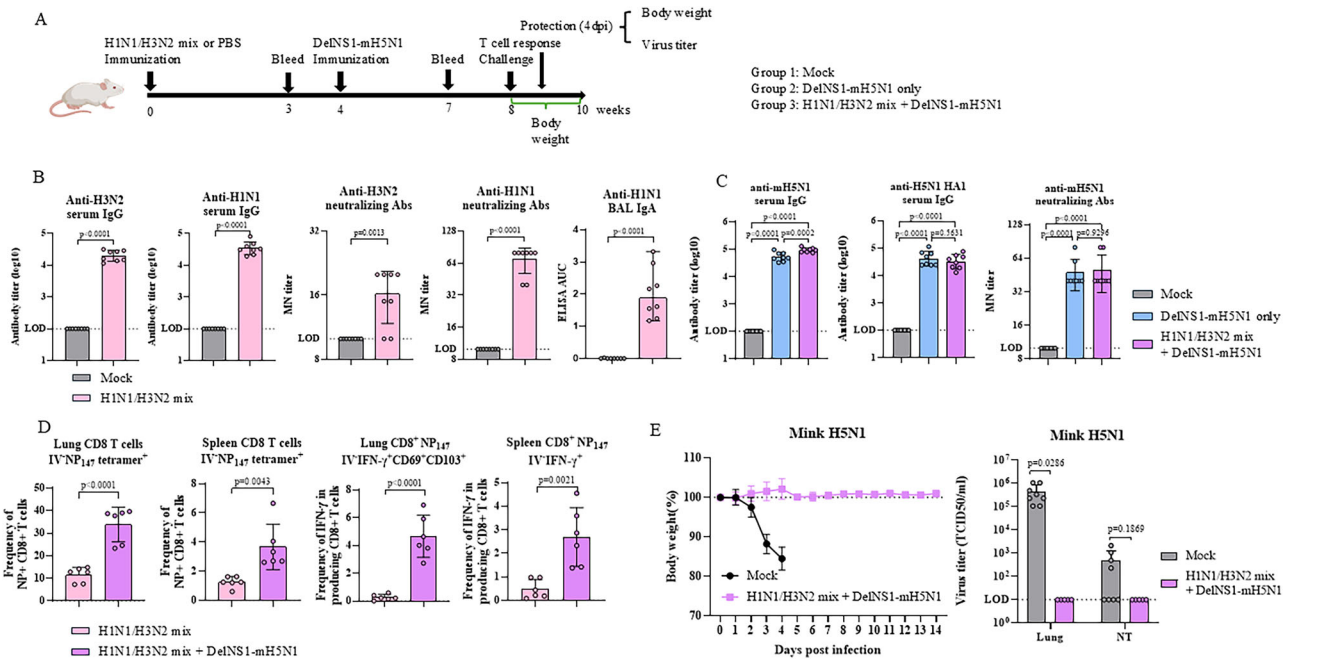

Fig. 6 | Effect of pre-existing immunity on the immunogenicity and protective ability of DelNS1-H5N1 vaccine. A Schedule of immunization, serum collection, T cell response, virus challenge and sacrifice for BALB/c mice. Mice were intranasally vaccinated with H1N1/H3N2 mix (10^6 pfu mixture of H3N2 and H1N1 DelNS1 LAIVs (1:1), $n = 23$), or mock-vaccinated ($n = 8$). 4 weeks after immunization, 15 mice from H1N1/H3N2 mix group and 8 mice from mock group were vaccinated with DelNS1-mH5N1 (10^6 pfu). Mice were challenged with mink H5N1 virus (10^4 pfu) 4 weeks later. **B** Serum was collected at week 3 post H1N1/H3N2 mix immunization and tested for IgG titers against H3N2 and H1N1 DelNS1 LAIVs and micro-neutralization titers against live viruses ($n = 8$ each group). BAL IgA level against H1N1 DelNS1 LAIVs were measured 8 weeks after H1N1/H3N2 mix vaccination ($n = 8$ each group). **C** Serum were collected 3 weeks after DelNS1-mH5N1 immunization and tested for IgG titers against live virus or H5N1-HA1 protein and micro-neutralization titers against live virus ($n = 8$ each group). **D** 8 weeks after prime immunization, for the H1N1/H3N2 mix group and H1N1/H3N2 mix + DelNS1-mH5N1 group ($n = 6$), PE-Cy5 CD45 antibody was injected intravenously 5 min before sacrifice. Lung cells and splenocytes were stained with Zombie, anti-CD8 and NP_{147} tetramer. The frequency of IV-CD8 + NP_{147} tetramer out of all live IV-CD8 T cells was displayed. Lung cells and splenocytes were stimulated with NP_{147} and stained with surface markers, followed by fixation, permeabilization, and intracellular staining for IFN-γ. The frequency of tissue-resident memory cells in lungs (IV-IFNγ+CD69+CD103+ CD8+ T cells out of all live IV-CD8 T cells) and spleens (IV-IFNγ+CD8+ T cells out of all live IV-CD8 T cells) was displayed. **E** 8 weeks after prime immunization, mice in H1N1/H3N2 mix + DelNS1-mH5N1 group ($n = 9$) and mock group ($n = 8$, two independent experiments) were challenged with mink H5N1 virus (10^4 pfu); body weights were monitored for 14 days, and viral titers in lungs and NT were measured at 4 dpi. LOD: limit of detection. Data represent mean values ± SD of results. Statistical analysis was performed using Student's *t*-test (two-tailed) (**B**, **D**, **E**) and one-way ANOVA (**C**). The mouse cartoon was created in BioRender. Wang, P. (2025) https://BioRender.com/n83i107. Source data are provided as a Source Data file.

models[23]. A pandemic vaccine administered via muscular injection may require at least two doses to generate adequate immunity against H5N1 infection and prevent disease in immunologically naive populations, as seen by COVID-19 vaccination efforts. An mRNA vaccine for H5N1 also demonstrated that two doses are necessary to induce sufficient immunity to protect against lethal challenge in ferrets[37]. In the event of a human outbreak with a highly virulent pathogen like the H5N1 virus, a vaccine that can rapidly induce antiviral immunity is crucial. The NS1 protein of the influenza virus is a potent immune antagonist and interferes with the host immune response to viral infection[39]. In the absence of NS1, the DelNS1 LAIV replicates natural infection and, more importantly, acts as a superior immunogen for eliciting full-spectrum anti-influenza immunity[23,40–43]. Our data showed that one dose of DelNS1-H5N1 induces a high level of systemic neutralizing antibodies, local mucosal IgA and tissue-resident memory T cells in immunized mice. Immunized mice show no loss of body weight, no apparent pathological changes, no induction of inflammatory cytokines in the lungs, and most importantly, no virus replication in the nasal turbinate after exposure to a lethal dose of the H5N1 virus.

Challenges exist in developing effective mucosal vaccines for respiratory viruses. The understanding of mucosal immunity is incomplete, and there is a lack of standardization in measuring mucosal immunity. It is also crucial to establish mucosal immune correlates to protection in humans. Testing technologies for developing mucosal vaccines for respiratory viruses in response to potential future pandemics has high significance[44,45]. Given the annual epidemic of influenza, combining vaccines with flu immunization would be an ideal strategy. The DelNS1-RBD, an intranasal spray vaccine based on the DelNS1 LAIV system that contains a COVID-19 receptor binding domain (RBD) sequence, has undergone evaluation for safety and efficacy in human clinical trials[46,47]. While the efficacy of using DelNS1-RBD LAIV for COVID-19 in a Phase III trial study was found to be low[47], there are several reasons that may explain why the vaccine efficacy was underwhelming in this clinical trial. One major factor could be that during the Phase III trial, the Omicron variant was the predominant circulating strain, whereas the vaccine tested utilized the RBD derived from the original strain (early SARS-CoV-2). We also recognize that the DelNS1-RBD used in the clinical trial was our first version of the DelNS1-RBD vaccine, developed in 2020. We have since made several optimizations and significantly improved the DelNS1-RBD LAIV vaccine system for expressing viral antigens[24]. It is also worth noting that utilizing DelNS1 LAIV as a vector to express another viral antigen (DelNS1-RBD expresses RBD from the deleted NS1 site) may be less efficient than when the virus expresses its own genes, such as HA and NA. DelNS1-H5N1 LAIV has demonstrated highly immunogenic properties and optimal protective efficacy, even at low doses, indicating its ability to generate optimal immunity against highly pathogenic avian H5N1 virus infection. While a major outbreak or pandemic in humans caused by H5N1 may be avoided through surveillance and early intervention to prevent further human transmission, the DelNS1 LAIV vaccine system

https://doi.org/10.1038/s41467-025-58504-z

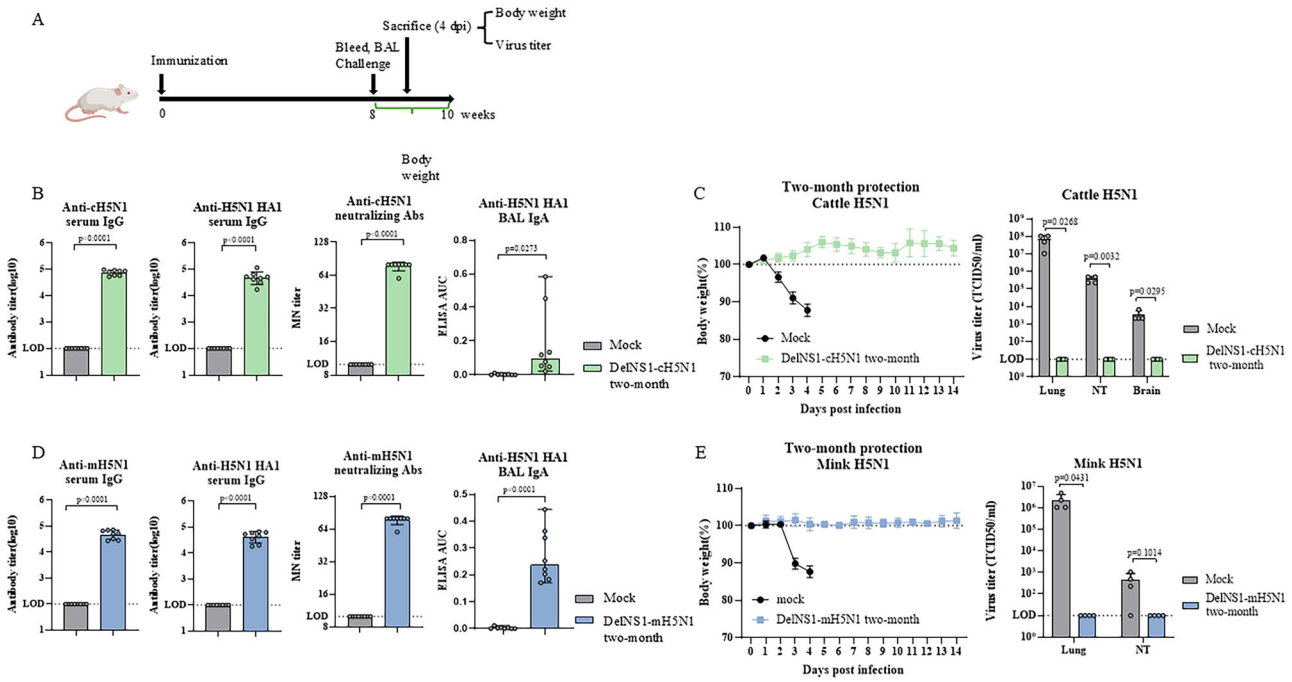

Fig. 7 | Effective protection after two-month DelNS1-H5N1 immunization. **A** Illustration of schedule of immunization, virus challenge and sacrifice for BALB/c mice. Mice were intranasally vaccinated with DelNS1-cH5N1 (10^6 pfu, $n = 16$) or mock-vaccinated ($n = 12$). **B** Serum was collected at week 8 and tested for IgG titers against cH5N1 (DelNS1-cH5N1) virus or H5N1-HA1 protein and micro-neutralization titers against live viruses. Levels of IgA against H5N1-HA1 in BAL were measured at week 8 following DelNS1-mH5N1 vaccination. **C** At 8 weeks after immunization, mice were challenged with cattle H5N1 virus (5000 pfu); body weights were monitored for 14 days and viral titers in the lungs, NT and brain were measured at 4 dpi ($n = 4$ for mock group; $n = 8$ for DelNS1-cH5N1 two-month group). **D** Mice were intranasally vaccinated with DelNS1-mH5N1 (10^6 pfu, $n = 16$) or mock-vaccinated ($n = 12$), and serum collected at week 8 tested for IgG titers against mH5N1 (DelNS1-mH5N1) virus or H5N1-HA1 protein and micro-neutralization titers against live virus. BAL levels of IgA recognizing H5N1-HA1 were measured at week 8 after DelNS1-mH5N1 vaccination. **E** Eight weeks after immunization, mice were challenged with mink H5N1 virus (10^4 pfu); body weights were monitored for 14 days and viral titers in the lungs and NT were measured at 4 dpi ($n = 4$ for mock group; $n = 8$ for DelNS1-mH5N1 two-month group). LOD limit of detection. Data represent mean values ± SD of results. Statistical analysis was performed using Student's *t*-test (two-tailed). Mouse cartoon was created in BioRender. Wang, P. (2025) https://BioRender.com/n83i107. Source data are provided as a Source Data file.

could also be crucial for future responses to other emerging influenza viruses due to its proved safety, ease of production, and the unique ability to effectively induce both systemic and mucosal immunity. In the pandemic preparedness and the response to seasonal epidemics, the DelNS1 influenza viral vector system has the potential to be a valuable vaccine platform for controlling of epidemics and preparing responses to emerging respiratory viruses. Further studies to evaluate these DelNS1-H5N1 vaccine candidates in humans are essential.

Methods

Cells and viruses

All cell lines in this study were procured from ATCC: MDCK (CCL34), A549 (CCL-185), and 293T (CRL-3216). Human embryonic kidney cells (293T) and lung adenocarcinoma cells (A549) were grown in Dulbecco's minimal essential medium (DMEM), enriched with 10% fetal bovine serum, 100 units/ml penicillin, and 100 µg/ml streptomycin sulfate (Life Technologies). Canine MDCK cells were cultivated in Eagle's minimal essential medium (MEM), supplemented with identical quantities of serum and antibiotics. Three strains of influenza viruses, H1N1 virus A/California/04/2009, H5N1 virus A/dairy cattle/Texas/24-008749-003-original/2024, and A/mink/Spain/22VIR12774-14_3869-3/2022, were rescued using reverse genetics[48,49]. Additionally, two DelNS1-H5N1 LAIVs were created, employing HA and NA from the H5N1 viruses. Three amino acids (RKR) were deleted from the polybasic cleavage motif (KRRKR↓GLF) in the hemagglutinin (HA) protein to attenuate the DelNS1-H5N1 LAIVs. All LAIVs were constructed and rescued according to the protocols described here and in our previous report[38]. The viral gene segments underwent amplification and were subsequently cloned into pHW2000 plasmids, resulting in eight pHW2000 plasmids. These plasmids were transfected into mixtures of 293T/MDCK cells, and the rescued virus was amplified in either MDCK cells or embryonated chicken eggs. For the pre-existing immunity experiment, the H3N2 and H1N1 DelNS1 LAIVs were derived from A/Guangdong-Maonan/SWL1536/2019 (H1N1) and A/HongKong/2671/2019 (H3N2).

Generation and passage of DelNS1 viruses

293T/MDCK cells were transfected with eight pHW2000 plasmids, containing the DelNS1 segment and the other seven influenza virus genomic segments. In addition, an NS1 expression plasmid was added. After incubating overnight, the DNA mixture was removed, and MEM with 1 µg/ml N-tosyl-L-phenylalanine chloromethyl ketone (TPCK)-treated trypsin (Sigma) was added. The virus supernatant was collected 72 h later and labeled as passage 0 (P0) virus. It was then passaged in MDCK cells or embryonated chicken eggs. For the H5N1 reassortant DelNS1 viruses DelNS1-cH5N1 and DelNS1-mH5N1, six plasmids containing CA4-DelNS1 internal genes and H5N1 HA and NA plasmids derived from either A/dairy cattle/Texas/24-008749-003-original/2024 virus or A/mink/Spain/22VIR12774-14_3869-3/2022 virus were utilized for virus rescue. To confirm the deletion of the NS1 gene in all DelNS1 viruses, reverse transcription-PCR (RT-PCR) and sequencing were performed.

Growth kinetics and stability test

Confluent MDCK or A549 cells in 24-well plates were infected with viruses at specific multiplicities of infection (MOI). Following a one-

hour adsorption period, the viral supernatant was removed. The cells were then washed twice with phosphate-buffered saline (PBS) and overlaid with MEM containing 1 μg/ml TPCK-treated trypsin. Cells were subsequently incubated at the temperatures indicated. Supernatants were collected at various time points, and titers were determined using plaque assays in MDCK cells. For the growth study in eggs, 8-day-old embryonated chicken eggs were infected with viruses at 7×10^4 pfu or 7×10^5 pfu, viruses were collected at 48 h post infection, and titers were determined using plaque assays in MDCK cells.

For the genetic stability test of DelNS1-cH5N1 and DelNS1-mH5N1 viruses, the rescued virus passage 0 (P0) DelNS1 viruses, DelNS1-cH5N1 and DelNS1-mH5N1were serially passaged 10 times at 33 °C in 9-day-old chicken embryonated eggs to evaluate their genetic stability. After each passage, viruses were diluted 100-fold in PBS and the passage was repeated. Following multiple passages (P5 and P10), viral RNA was extracted by viral RNA extraction kit (Qiagen). cDNA was synthesized using the High-Capacity cDNA reverse transcription kit (Invitrogen) and uni-12 primer. Viral genes were amplified by PCR using gene-specific primers, as detailed in the Supplementary Data 1 file. The complete genomes of the DelNS1 viruses were subsequently sequenced using the Sanger method to identify any potential mutations. Whole genome sequences were summited to GenBank (GenBank accession numbers: DelNS1-mH5N1-p1: PV124973-PV124980, DelNS1-mH5N1-p10: PV124993-PV125000).

Plaque assay and $TCID_{50}$ assay

For plaque assay, viruses were serially diluted by a factor of 10 and then added to confluent MDCK cells in 6-well plates. These plates were then incubated at 37 °C for one hour. After this, the supernatant was discarded, and the cells were washed twice with PBS. Next, the cells were overlaid with 1% MEM agarose that contained 1 μg/ml TPCK-treated trypsin. The plates were then incubated at a temperature of 33 °C for a period of 48 h. Following this incubation period, the plates were fixed with a 10% PBS-buffered formaldehyde solution for a minimum of 2 h. Finally, plaques were made visible by staining with a 1% crystal violet solution.

For $TCID_{50}$ assay, confluent MDCK cells in 96 well plates were washed and overlaid with MEM containing 1 μg/ml TPCK-treated trypsin, and then incubated with serially diluted virus. After 3 days, the presence of virus was detected by HA assay. $TCID_{50}$ values were calculated by the Reed–Muench Method.

Animal immunization and challenge

For mouse immunization, 6–8-week-old female BALB/c mice were anesthetized with ketamine and xylazine and then immunized intranasally with 2×10^5 pfu (low titer dose, Fig. S7) or 1×10^6 pfu (standard dose, all other experiments) of DelNS1-H5N1 LAIV vaccine. Three weeks after the immunization, blood serum was collected for ELISA and microneutralization assays. At week 4, mice were euthanized and bronchoalveolar lavage fluid (BAL), nasal washes, lungs and spleens were collected for ELISA and T cell response assays.

To determine the mouse lethal dose 50 (LD_{50}), 6–8-week-old female BALB/c mice were anesthetized with ketamine and xylazine and then intranasally inoculated with 20 μl of different titers of cattle H5N1 ($n = 4$ for each group; 5000 pfu, 500 pfu, 50 pfu, 5 pfu, <1 pfu), or intranasally inoculated with 20 μl of different titers of mink H5N1 ($n = 4$ for each group; 10^4 pfu, 10^3 pfu, 10^2 pfu, 10 pfu). Body weight and survival were monitored daily for 15 days. The mice were euthanized if they lost more than 20% of their initial body weight. LD_{50} values were calculated based on the Reed-Muench method[50].

For virus challenge, after 4 weeks immunized mice were challenged intranasally with H5N1 virus (cattle H5N1: 5×10^3 pfu, mink H5N1: 1×10^4 pfu). Body weight and disease signs were monitored daily. At day 4 post infection, lungs and nasal turbinates (NT) or other organs were collected for virus titration and histopathological and immunohistochemical study and the remaining challenged mice were monitored for body weight and disease signs. For the virus titer detection, the collected organs (whole organ) were homogenized in 1 ml PBS, centrifuged and supernatants were then used for virus titration using $TCID_{50}$ assay (virus titters were calculated as $TCID_{50}$/ml). For the pre-existing immunity and immunity longevity studies immunization, sampling, challenge and sacrifice timings were adjusted, as detailed in the relevant sections.

For hamster immunization, 6–8-week-old male hamsters (Golden Syrian Hamster) were anesthetized with ketamine and xylazine and then immunized intranasally with 5×10^6 pfu of DelNS1-cH5N1 LAIV vaccine. Three weeks after the immunization, blood serum was collected for ELISA and microneutralization assays. For virus challenge, after 4 weeks immunized hamsters were challenged intranasally with H5N1 virus (cattle H5N1, 1×10^4 pfu). Body weight and disease signs were monitored daily. At 4 days post infection, lungs and nasal turbinates (NT) or other organs were collected for virus titration and the remaining challenged hamsters were monitored for body weight and disease symptoms. For the virus titer detection, the collected organs were then homogenized in 2 ml PBS, then centrifuged and supernatants were used for virus titration using $TCID_{50}$ assay.

All animal experiments were approved by the Committee on the Use of Live Animals in Teaching and Research of the University of Hong Kong (HKU) (CULATR) (# 22-092). All animal experiments related to H5N1 were performed in a biosafety level 3 laboratory at HKU. Animals were housed and bred under an AAALAC International accredited program at the Center for Comparative Medicine Research (CCMR), The University of Hong Kong. Animals were housed in open cages or individually ventilated cages under a 12:12 dark/light cycle within environmentally controlled rooms. Standard pellet feed and water were provided ad libitum.

Microneutralization (MN) assays

Serum from immunized BALB/c mice were treated with receptor-destroying enzyme (RDE; Denka Seiken). RDE-treated serum was then twofold serially diluted in 96-well plates and mixed with 100 50% tissue culture infective doses ($TCID_{50}$) of virus, then incubated for 1 h at room temperature. The mixture was added to confluent MDCK cells in MEM supplemented with 1 μg/ml TPCK-treated trypsin in a 96-well plate and incubated at 33 °C for 3 days. The presence of virus was confirmed by hemagglutination (HA) assay. The neutralizing titer was defined as the reciprocal of the highest dilution of serum that completely neutralizes infectivity of 100 $TCID_{50}$ of virus in MDCK cells.

Enzyme-linked immunosorbent assay (ELISA)

DelNS1-cH5N1 (4×10^5 pfu/well), DelNS1-mH5N1 (4×10^5 pfu/well), H5N1 HA1 (100 ng/well) (A/chicken/Ghana/AVL-763_21VIR7050-39/2021, Sino Biological 40933-V08B), the H3N2 DelNS1 LAIVs (4×10^5 pfu/well), or the H1N1 DelNS1 LAIVs (4×10^5 pfu/well) was coated onto MaxiSorp 96-well plates (Thermo Scientific) at 4 °C overnight. Plates were washed with PBS and blocked with 3% BSA at room temperature for 1 h. For serum IgG detection, heat-inactivated serum was tenfold serially diluted and added to the plate, then incubated at 37 °C for 30 min. For the detection of IgA in bronchoalveolar lavage fluid (BAL) or nasal washes, BAL and nasal washes were diluted fivefold and tenfold, respectively, in PBST, then undiluted or diluted BAL and nasal washes were added to the plate and incubated at 37 °C for 30 min. The plate was washed 5 times and then incubated with secondary antibody reagent at 37 °C for 30 min. After washing, color development solution was added and incubated at 37 °C for 15 min. Stop solution was added and absorbance at 450 nm was measured using a Varioskan LUX Multimode Microplate Reader (ThemoFisher). The endpoint for serum IgG detection and the area under the curve (AUC) for IgA detection were calculated using GraphPad Prism v10.

Intracellular cytokine staining (ICS) and NP_{147} tetramer staining

To study tissue-resident memory T cells, 4 weeks after immunization, and following intravascular labeling by using injection of anti-CD45-PE-Cy5 (Biolegend-103110, Clone-30-F11, Lot-B392814) at the dose of 2 μg per mouse, 5 min prior to sacrifice, lungs and spleens of mice were collected. Splenocytes were isolated and homogenized through cell strainers (BD) and resuspended in RPMI medium (10% FBS and P/S). Lung tissue was chopped and digested in RPMI solution with Collagenase D (1 mg/ml) (Roche) for 1 h at 37 °C. Red blood cells were lysed by addition of Lysing solution (BD). After washing with RPMI, cells were counted and resuspended in RPMI. Cells were stimulated with RPMI solution containing influenza A virus-NP147 or -NP55 peptide at a final working concentration of 1 μg/ml per peptide (GenScript, NP147-TYQRTRALV, NP55-RLIQNSITIERMVLS). After 1 h, brefeldin A (BFA) was added to cells and incubated overnight. Cells were then washed with FACS buffer (2% FBS in PBS) and stained with Zombie (BioLegend-423102, Lot-B432360), anti-CD8-AF700 (BioLegend-100730, Clone-53-6.7, Lot-B433204), anti-CD4-FITC (BioLegend-100406, Clone-GK1.5, Lot-B374032), anti-CD69-BV711 (BioLegend-104537, Clone-H1.2F3, Lot-B406939) and CD103-BV421 (BioLegend-121422,Clone-2E7, Lot-B425334) for 30 min at 4 °C. Cells were washed and fixed with Perm/wash buffer (BD), and then stained with anti-IFNγ-APC (BioLegend-505810, Clone-XMG1.2, Lot-B335090) overnight at 4 °C. Cells were then washed twice with FACS buffer and resuspended in FACS buffer. For NP_{147} tetramer staining, after IV labeling and isolation of cells from tissues, lung cells and splenocytes were stained with Zombie (BioLegend-423102, Lot-B432360), anti-CD8-BV785 (BioLegend-100750, Clone-53-6.7, Lot-B420449) and NP_{147} tetramer-APC (MBL International-TB-M534-2, Lot-T2405016) for 30 min at 4 °C. Cells were washed and finally resuspended in FACS buffer. The samples were acquired with an Agilent NovoCyte Quanteon analyzer, and the generated data analyzed with FlowJo V10. Cytokine production was calculated by subtracting the no peptide control background value. The gating strategy is shown in Fig. S8.

RNA isolation and RT-qPCR

Total RNA was isolated from BALB/c mouse lungs using RNAzol RT reagent (MRC) according to the manual, and first-strand cDNA was generated from total RNA using HiScript III All-in-one RT SuperMix Perfect for qPCR (Vazyme) following the protocol provided. Real-time PCR was conducted with the TB Green Premix Ex Taq II (Takara) and gene-specific primers on a LightCycler® 480 System (Roche). PCR conditions were as follows: initial denaturation: 95 °C for 30 s, 40 cycles of amplification: 95 °C for 10 s, 60 °C for 10 s, 72 °C for 10 s, and melting curve analysis: 65 °C to 97 °C at 0.1 °C/s. Expression of target genes was normalized to internal reference genes (mouse β-Actin) and the comparative Ct method utilized to calculate the cytokine expression profile. All the primers have been described previously and showed in the Supplementary Data 1 file[51].

Histopathology

Following fixation in 10% PBS buffered formalin, organs of infected BALB/c mice and Golden Syrian Hamsters were processed into paraffin blocks. Haematoxylin and eosin (H&E) staining was performed on tissue sections and subsequently examined under light microscopy. Pathological scores were given based on the pathological changes observed in the tissues according to a previous report[52].

Immunohistochemistry

Formalin-fixed paraffin-embedded lung sections, nasal turbinate sections and brain sagittal sections of infected BALB/c mice and Golden Syrian Hamsters were labelled for immunohistochemical staining using a rabbit polyclonal anti-influenza A virus nucleoprotein antibody (GeneTex-GTX125989, Lot-44902). Briefly, sections were deparaffinized and rehydrated. Heat-induced epitope retrieval was performed using Antigen Unmasking Solution, Tris-Based (Vector Laboratories, H-3301-250) in a pressure cooker for about 1 min once the cooker had pressurized. Sections were then incubated with hydrogen peroxide to inactivate endogenous peroxidase activities prior to applying the primary antibody (1:2000) at 4 °C overnight, followed by a secondary antibody (Dako EnVision+ System- HRP Labelled Polymer Anti-Rabbit, Agilent-K4003) for 30 min at room temperature. Diaminobenzidine chromogen detection was completed using Dako DAB for 2 min (Agilent-K3468). Sections were then rinsed with deionized water and counterstained using hematoxylin. Finally, slides were cleared through a gradient of alcohol and xylene prior to mounting and coverslipping. Sections were examined under a light microscope.

Statistical analysis

Statistical analysis was carried out using GraphPad Prism. Data were presented as the mean values ± SD of at least 3 replicates. Statistical significance was analyzed by either Student's *t*-test or one-way analysis of variance (ANOVA) followed by Dunn's multiple comparisons test. For all tests: $^{****}p < 0.0001$, $^{***}p < 0.001$, $^{**}p < 0.01$, $^{*}p < 0.05$, ns-not significant.

Reporting summary

Further information on research design is available in the Nature Portfolio Reporting Summary linked to this article.

Data availability

All data associated with this study are presented within the paper or in the Supplementary materials. For the genetic stability test of DelNS1-cH5N1 and DelNS1-mH5N1 viruses, whole genome sequences were summited to GenBank (GenBank accession numbers: DelNS1-mH5N1-p1: PV124973-PV124980, DelNS1-mH5N1-p10: PV124993-PV125000). Raw data underling the results are provided with this paper. Source data are provided with this paper.

References

1. Yuen, K. Y. et al. Clinical features and rapid viral diagnosis of human disease associated with avian influenza A H5N1 virus. *Lancet* **351**, 467–471 (1998).
2. Li, K. S. et al. Genesis of a highly pathogenic and potentially pandemic H5N1 influenza virus in eastern Asia. *Nature* **430**, 209–213 (2004).
3. Chen, H. et al. Establishment of multiple sublineages of H5N1 influenza virus in Asia: implications for pandemic control. *Proc. Natl Acad. Sci. USA* **103**, 2845–2850 (2006).
4. Chen, H. et al. Avian flu: H5N1 virus outbreak in migratory waterfowl. *Nature* **436**, 191–192 (2005).
5. Lee, D. H., Bertran, K., Kwon, J. H. & Swayne, D. E. Evolution, global spread, and pathogenicity of highly pathogenic avian influenza H5Nx clade 2.3.4.4. *J. Vet. Sci.* **18**, 269–280 (2017).
6. Xie, R. et al. The episodic resurgence of highly pathogenic avian influenza H5 virus. *Nature* **622**, 810–817 (2023).
7. Aguero, M. et al. Highly pathogenic avian influenza A(H5N1) virus infection in farmed minks, Spain, October 2022. *Euro Surveill* **28**. https://doi.org/10.2807/1560-7917.ES.2023.28.3.2300001 (2023).
8. Caserta, L. C. et al. Spillover of highly pathogenic avian influenza H5N1 virus to dairy cattle. *Nature*. https://doi.org/10.1038/s41586-024-07849-4 (2024).
9. Kandeil, A. et al. Rapid evolution of A(H5N1) influenza viruses after intercontinental spread to North America. *Nat. Commun.* **14**, 3082 (2023).
10. Mellis, A. M. et al. Serologic Evidence of Recent Infection with Highly Pathogenic Avian Influenza A(H5) Virus Among Dairy Workers - Michigan and Colorado, June-August 2024. *MMWR Morb. Mortal. Wkly Rep.* **73**, 1004–1009 (2024).

11. Tosheva, I. I. et al. Influenza A(H5N1) shedding in air corresponds to transmissibility in mammals. *Nat Microbiol*. https://doi.org/10.1038/s41564-024-01885-6 (2024).
12. Eisfeld, A. J. et al. Pathogenicity and transmissibility of bovine H5N1 influenza virus. *Nature*. https://doi.org/10.1038/s41586-024-07766-6 (2024).
13. Lin, T. H. et al. A single mutation in bovine influenza H5N1 hemagglutinin switches specificity to human receptors. *Science* **386**, 1128–1134 (2024).
14. Good, M. R. et al. A single mutation in dairy cow-associated H5N1 viruses increases receptor binding breadth. *Nat. Commun.* **15**, 10768 (2024).
15. Jassem, A. N. et al. Critical illness in an adolescent with influenza A(H5N1) virus infection. *N. Engl. J. Med*. https://doi.org/10.1056/NEJMc2415890 (2024).
16. Chen, Y. et al. Human infections with the emerging avian influenza A H7N9 virus from wet market poultry: clinical analysis and characterisation of viral genome. *Lancet* **381**, 1916–1925 https://doi.org/10.1016/S0140-6736(13)60903-4.
17. Lam, T. T. et al. Dissemination, divergence and establishment of H7N9 influenza viruses in China. *Nature* **522**, 102–105 (2015).
18. Shi, J., Zeng, X., Cui, P., Yan, C. & Chen, H. Alarming situation of emerging H5 and H7 avian influenza and effective control strategies. *Emerg. Microbes Infect.* **12**, 2155072 (2023).
19. Wang, X. et al. Epidemiology of avian influenza A H7N9 virus in human beings across five epidemics in mainland China, 2013-17: an epidemiological study of laboratory-confirmed case series. *Lancet Infect. Dis.* **17**, 822–832 (2017).
20. Kumar, M., Chu, H. J., Rodenberg, J., Krauss, S. & Webster, R. G. Association of serologic and protective responses of avian influenza vaccines in chickens. *Avian Dis.* **51**, 481–483 (2007).
21. Kim, J. K. et al. Puzzling inefficiency of H5N1 influenza vaccines in Egyptian poultry. *Proc. Natl. Acad. Sci. USA* **107**, 11044–11049 (2010).
22. Tregoning, J. S., Flight, K. E., Higham, S. L., Wang, Z. & Pierce, B. F. Progress of the COVID-19 vaccine effort: viruses, vaccines and variants versus efficacy, effectiveness and escape. *Nat. Rev. Immunol.* **21**, 626–636 (2021).
23. Wang, P. et al. Generation of DelNS1 influenza viruses: a strategy for optimizing live attenuated influenza vaccines. *mBio* **10**. https://doi.org/10.1128/mBio.02180-19 (2019)
24. Deng, S. et al. An intranasal influenza virus-vectored vaccine prevents SARS-CoV-2 replication in respiratory tissues of mice and hamsters. *Nat. Commun.* **14**, 2081 (2023).
25. Hu, X. et al. Genomic characterization of highly pathogenic avian influenza A H5N1 virus newly emerged in dairy cattle. *Emerg. Microbes Infect.* **13**, 2380421 (2024).
26. Burrough, E. R. et al. Highly pathogenic avian influenza A(H5N1) Clade 2.3.4.4b virus infection in domestic dairy cattle and cats, United States, 2024. *Emerg. Infect. Dis.* **30**, 1335–1343 (2024).
27. Khurana, S. et al. Licensed H5N1 vaccines generate cross-neutralizing antibodies against highly pathogenic H5N1 clade 2.3.4.4b influenza virus. *Nat. Med.* **30**, 2771–2776 (2024).
28. Apps, R. et al. Acute and persistent responses after H5N1 vaccination in humans. *Cell Rep.* **43**, 114706 (2024).
29. Lasrado, N. et al. SARS-CoV-2 XBB.1.5 mRNA booster vaccination elicits limited mucosal immunity. *Sci. Transl. Med.* **16**, eadp8920 (2024).
30. Declercq, J. et al. Repeated COVID-19 mRNA-based vaccination contributes to SARS-CoV-2 neutralizing antibody responses in the mucosa. *Sci. Transl. Med.* **16**, eadn2364 (2024).
31. Beigel, J. H. et al. Avian influenza A (H5N1) infection in humans. *N. Engl. J. Med.* **353**, 1374–1385 (2005).
32. de Jong, M. D. et al. Fatal outcome of human influenza A (H5N1) is associated with high viral load and hypercytokinemia. *Nat. Med.* **12**, 1203–1207 (2006).
33. Peacock, T. P. et al. The global H5N1 influenza panzootic in mammals. *Nature* **637**, 304–313 (2025).
34. Altmann, D. M. & Boyton, R. J. COVID-19 vaccination: The road ahead. *Science* **375**, 1127–1132 (2022).
35. Subbarao, K., Murphy, B. R. & Fauci, A. S. Development of effective vaccines against pandemic influenza. *Immunity* **24**, 5–9 (2006).
36. Subbarao, K. The success of SARS-CoV-2 vaccines and challenges ahead. *Cell Host Microbe* **29**, 1111–1123 (2021).
37. Hatta, M. et al. An influenza mRNA vaccine protects ferrets from lethal infection with highly pathogenic avian influenza A(H5N1) virus. *Sci. Transl. Med.* **16**, eads1273 (2024).
38. Zheng, M. et al. An A14U Substitution in the 3′ Noncoding Region of the M Segment of Viral RNA Supports Replication of Influenza Virus with an NS1 deletion by modulating alternative splicing of M segment mRNAs. *J. Virol.* **89**, 10273–10285 (2015).
39. Klemm, C., Boergeling, Y., Ludwig, S. & Ehrhardt, C. Immunomodulatory nonstructural proteins of influenza A Viruses. *Trends Microbiol* **26**, 624–636 (2018).
40. Fernandez-Sesma, A. et al. Influenza virus evades innate and adaptive immunity via the NS1 protein. *J. Virol.* **80**, 6295–6304 (2006).
41. Pica, N., Langlois, R. A., Krammer, F., Margine, I. & Palese, P. NS1-truncated live attenuated virus vaccine provides robust protection to aged mice from viral challenge. *J. Virol.* **86**, 10293–10301 (2012).
42. Richt, J. A. & Garcia-Sastre, A. Attenuated influenza virus vaccines with modified NS1 proteins. *Curr. Top. Microbiol. Immunol.* **333**, 177–195 (2009).
43. Mueller, S. N., Langley, W. A., Carnero, E., Garcia-Sastre, A. & Ahmed, R. Immunization with live attenuated influenza viruses that express altered NS1 proteins results in potent and protective memory CD8+ T-cell responses. *J. Virol.* **84**, 1847–1855 (2010).
44. Morens, D. M., Taubenberger, J. K. & Fauci, A. S. Rethinking next-generation vaccines for coronaviruses, influenzaviruses, and other respiratory viruses. *Cell Host Microbe* **31**, 146–157 (2023).
45. Lavelle, E. C. & Ward, R. W. Mucosal vaccines - fortifying the frontiers. *Nat. Rev. Immunol.* **22**, 236–250 (2022).
46. Zhu, F. et al. Safety and immunogenicity of a live-attenuated influenza virus vector-based intranasal SARS-CoV-2 vaccine in adults: randomised, double-blind, placebo-controlled, phase 1 and 2 trials. *Lancet Respir. Med.* **10**, 749–760 (2022).
47. Zhu, F. et al. Safety and efficacy of the intranasal spray SARS-CoV-2 vaccine dNS1-RBD: a multicentre, randomised, double-blind, placebo-controlled, phase 3 trial. *Lancet Respir. Med.* **11**, 1075–1088 (2023).
48. Hoffmann, E., Neumann, G., Kawaoka, Y., Hobom, G. & Webster, R. G. A DNA transfection system for generation of influenza A virus from eight plasmids. *Proc. Natl. Acad. Sci. USA* **97**, 6108–6113 (2000).
49. Song, W. et al. The K526R substitution in viral protein PB2 enhances the effects of E627K on influenza virus replication. *Nat. Commun.* **5**, 5509 (2014).
50. Reed, L. J. & Muench, H. A simple method of estimating fifty per cent endpoints12. *Am. J. Epidemiol.* **27**, 493–497 (1938).
51. Xia, X. et al. NLRX1 negatively regulates TLR-induced NF-κB signaling by targeting TRAF6 and IKK. *Immunity* **34**, 843–853 (2011).
52. Chen, Y. et al. COVID-19 mRNA vaccine protects against SARS-CoV-2 Omicron BA.1 infection in diet-induced obese mice through boosting host innate antiviral responses. *EBioMedicine* **89**, 104485 (2023).

Acknowledgements

This study was supported by Health@InnoHK, Innovation and Technology Commission (H.C., K.K-W.T. and K-Y.Y.) the Theme-Based Research Scheme (T11-709/21-N) (H.C), HMRF Commissioned Research (HMRF19181052) (H.C., K.K-W.T. and K-Y.Y.), Hong Kong Special Administrative Region, China, National Key Project (2021YFC0866100)

(H.C.), and the Emergency Collaborative Project (EKPG22-01) (H.C., K.K-W.T.) of Guangzhou Laboratory, China. The authors would like to thank Dr. Jane Rayner for critical reading and editing of the manuscript.

Author contributions

H.C. and P.W. conceived the studies; P.W., Y.L., S.D., S.R., R.C-Y.T., and S.L. performed experiments; P.W., Y.L., S.D., S.R., R.C-Y.T., A.J.Z., K.K-W.T., K-Y.Y., and H.C. analyzed and interpreted the data; H.C., P.W., and Y.L. wrote the paper.

Competing interests

The authors declare that the University of Hong Kong owns patents on work related to the generation and application of DelNS1 live attenuated influenza vaccines and the associated platform, with H.C., P.W. and K-Y.Y. included as co-inventors. There is no restriction on the publication of data. The other authors declare that they have no competing interests.

Additional information

Supplementary information The online version contains supplementary material available at https://doi.org/10.1038/s41467-025-58504-z.

Correspondence and requests for materials should be addressed to Honglin Chen or Pui Wang.

Peer review information *Nature Communications* thanks the anonymous reviewers for their contribution to the peer review of this work. A peer review file is available.